

Angiopep-2 Modified Exosomes Load Rifampicin with Potential for Treating Central Nervous System Tuberculosis

Han Li^{1,*}, Yinan Ding^{2,*}, Jiayan Huang¹, Yanyan Zhao¹, Wei Chen³, Qiusha Tang², Yanli An⁴, Rong Chen⁵, Chunmei Hu¹

¹Department of Tuberculosis, The Second Hospital of Nanjing, Nanjing University of Chinese Medicine, Nanjing, People's Republic of China; ²Medical School of Southeast University, Nanjing, People's Republic of China; ³Department of Clinical Research Center, The Second Hospital of Nanjing, Nanjing University of Chinese Medicine, Nanjing, People's Republic of China; ⁴Jiangsu Key Laboratory of Molecular and Functional Imaging, Department of Radiology, Zhongda Hospital, Medical School of Southeast University, Nanjing, People's Republic of China; ⁵Department of Oncology, Zhongda Hospital, Southeast University, Nanjing, Jiangsu, People's Republic of China

*These authors contributed equally to this work

Correspondence: Chunmei Hu, Department of tuberculosis, the Second Hospital of Nanjing, Nanjing University of Chinese Medicine, Nanjing, 210009, People's Republic of China, Email njyy003@njucm.edu.cn

Background: Central nervous system tuberculosis (CNS-TB) is the most devastating form of extrapulmonary tuberculosis. Rifampin (RIF) is a first-line antimicrobial agent with potent bactericidal action. Nonetheless, the blood-brain barrier (BBB) limits the therapeutic effects on CNS-TB. Exosomes, however, can facilitate drug movements across the BBB. In addition, exosomes show high biocompatibility and drug-loading capacity. They can also be modified to increase drug delivery efficacy. In this study, we loaded RIF into exosomes and modified the exosomes with a brain-targeting peptide to improve BBB permeability of RIF; we named these exosomes ANG-Exo-RIF.

Methods: Exosomes were isolated from the culture medium of BMSCs by differential ultracentrifugation and loaded RIF by electroporation and modified ANG by chemical reaction. To characterize ANG-Exo-RIF, Western blot (WB), nanoparticle tracking analysis (NTA) and transmission electron microscopy (TEM) were performed. Bend.3 cells were incubated with DiI labeled ANG-Exo-RIF and then fluorescent microscopy and flow cytometry were used to evaluate the targeting ability of ANG-Exo-RIF in vitro. Fluorescence imaging and frozen section were used to evaluate the targeting ability of ANG-Exo-RIF in vivo. MIC and MBC were determined through microplate alamar blue assay (MABA).

Results: A novel exosome-based nanoparticle was developed. Compared with untargeted exosomes, the targeted exosomes exhibited high targeting capacity and permeability in vitro and in vivo. The MIC and MBC of ANG-Exo-RIF were 0.25 µg/mL, which were sufficient to meet the clinical needs.

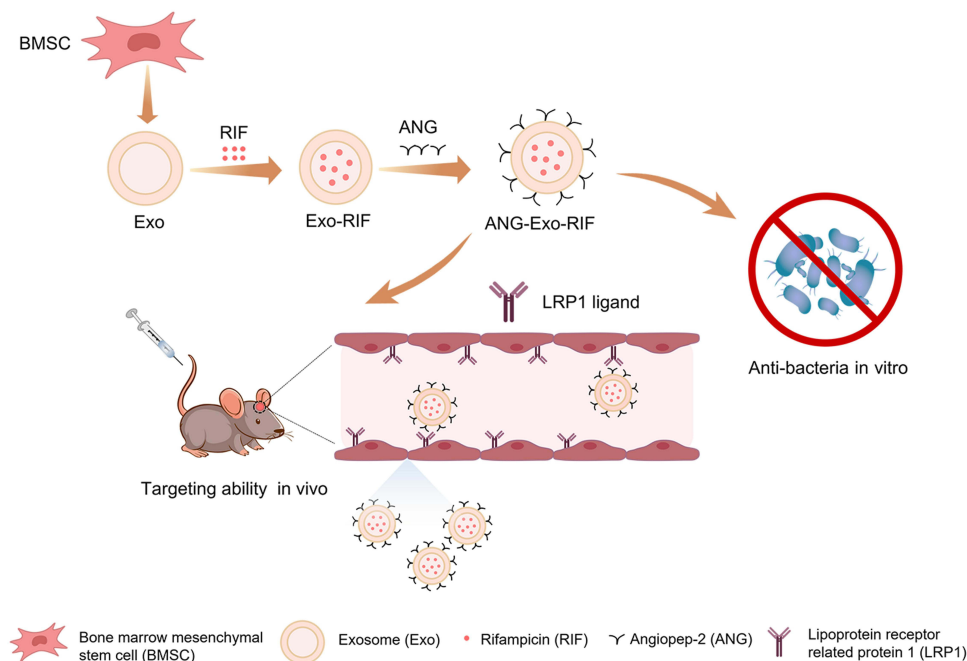
Conclusion: In summary, excellent targeting ability, high antitubercular activity and biocompatibility endow ANG-Exo-RIF with potential for use in future translation-aimed research and provide hope for an effective CNS-TB treatment.

Keywords: exosome, central nervous system tuberculosis, blood-brain barrier, rifampin

Introduction

Tuberculosis (TB) is an infectious disease caused by a mycobacterial infection. Central nervous system tuberculosis (CNS-TB) is the most devastating form of extrapulmonary tuberculosis with high mortality and disability rates.^{1,2} For example, tuberculous meningitis, a kind of CNS-TB, can lead to the death or neurological sequelae in one-half of the patients infected, including those taking anti-tuberculosis therapy.³ Rifampin (RIF), an inhibitor of DNA-dependent RNA polymerase, exhibits excellent antibacterial ability as a first-line TB drug.⁴ However, the blood-brain barrier (BBB) limits its permeability into affected areas.^{1,5} At the recommended dose of RIF, the ratio of the drug concentration in CSF to that in serum is 0.04–0.11; in the CSF, RIF at this

Graphical Abstract



concentration barely reaches the minimum inhibitory concentration (MIC) against mycobacterium tuberculosis.⁶ This indicates that the existence of the BBB leads to the low drug concentration in the brain, which greatly reduces the therapeutic efficiency. Therefore, improving the drug's ability to penetrate the BBB may be a promising and effective way to improve RIF-based therapy in CNS-TB.⁷ Recently, the strategy of nano-based drug delivery has been developed.⁸ Although the nano-based drug delivery systems can improve the therapeutic efficacy of drugs, the biosafety of the nanomaterials used for this purpose cannot be ignored.⁹ Therefore, better drug carriers need to be explored.

Exosomes, with a size range of 40–160nm, are lipid bilayer particles secreted by cells.^{10,11} Exosomes are important tool for cell-to-cell communication. During exosome formation, proteins, ribonucleic acids (RNAs) and other substances are encapsulated in exosomes and shuttled between cells, recognizing recipient cells by surface protein and then achieving information transfer.¹² As a natural carrier, exosomes show several excellent drug carrier characteristics. First, exosomes exhibit has high biocompatibility without inducing biotoxicity. Moreover, exosomes possess superior drug-loading capacity, which suggests that they are suitable as drug carriers.^{13,14} Most importantly, exosomes can cross the BBB.^{15,16} In summary, exosomes show the potential to be excellent nanodrug delivery carriers. Hopefully, some clinical trials will use exosomes as carriers for drug delivery.¹⁷ However, relevant studies have shown that natural exosomes cannot actively target the brain, with most of the exosomes accumulating in the liver and spleen. Therefore, in this study, we modified BBB-targeted peptides on the surface of exosomes to actively target to the brain. Among all the methods of modification, the most feasible method involves chemically connecting peptides to the surface of exosomes.^{18,19} Jia successfully used this method to confer exosomes targeting capacity in glioma therapy.¹⁹

Endothelial cells are the main components of the BBB, which prevents harmful substances and macromolecular drugs in the blood from entering the brain. Low-density lipoprotein receptor-related protein 1 (LRP1) is highly expressed on brain microvascular endothelial cells. The Angiopep-2 (TFYGGSRGKRNNFKTEEY, a 2.4 kDa protein, ANG) peptide can specifically recognize LRP1, and has shown the ability to target the BBB.^{20–22} Considering this information, we modified the surface of exosomes with ANG to target the BBB and increase the concentration of RIF in the brain.

An ANG-modified, RIF-loaded exosome (ANG-Exo-RIF) was designed for the treatment of CNS-TB. We chose exosomes derived from mesenchymal stem cells (MSCs) as drug carriers, which can promote tissue repair with low immunogenicity.^{23–25}

Then, we loaded RIF into the exosomes by electroporation.¹⁹ In addition, to solve the problem of low levels of drug delivery through the BBB, we modified ANG on the surface of the exosomes.^{26–28} After the preparation of ANG-Exo-RIF, targeting experiments *in vitro* and *in vivo* demonstrated that ANG-Exo-RIF can be preferentially delivered to the brain tissue and increase the concentration of drug in the brain. Additionally, ANG-Exo-RIF showed excellent antibacterial effects *in vitro*. Thus, use of ANG-Exo-RIF might act as a promising therapeutic strategy for CNS-TB in future clinical applications.

Materials and Methods

Cell Culture and Reagents

In this study, the bend.3 mouse brain microvascular endothelial cell line was purchased from Shanghai Zhongqiao Xinzhou Biotechnology Co., Ltd., and cultured in high glucose Dulbecco's modified Eagle's medium (DMEM) supplemented with 10% fetal bovine serum (FBS) and 1% penicillin and streptomycin. RIF was purchased from Sangon Biotech (Shanghai, China) Co., Ltd. The ANG-peptide (coupled with FITC) was purchased from the Chinese Peptide Company (Hangzhou, China). All other cell culture media and reagents were purchased from Gibco (Carlsbad, CA, USA). Cell culture plates and transwell chamber were obtained from NEST Biotechnology Co. Ltd (Wuxi, China).

Isolation of Bone Marrow Mesenchymal Stem Cells

Bone marrow mesenchymal stem cells (BMSCs) were isolated and cultured according to previous reports.²⁹ In brief, cells from 3 to 4-week-old C57BL/6 mice were collected by flushing the femurs and tibias with phosphate-buffered saline (PBS), and then, the cells were cultured in complete DMEM/F12 (containing 10% FBS and 1% penicillin and streptomycin). The cells were maintained in 37°C humidified incubator with 5% CO₂. To identify BMSCs, flow cytometry and differentiation assays were performed.

Isolation and Purification of Exosomes

According to previous reports, FBS was centrifuged at 110,000×g for 70 min to remove endogenous exosomes before it was used for cell culture at first.¹⁹ BMSCs were cultured in DMEM containing 10% Exo-free FBS, and the supernatant was collected and centrifuged sequentially to isolate exosomes. Briefly, the supernatant was centrifuged at 300×g for 10 min, 2000×g for 10 min and 10,000×g for 30 min to remove cells and cell debris. Then, the supernatant was ultracentrifuged at 110,000×g for 70 min to pellet exosomes. The exosomes were washed in PBS, ultracentrifuged at 110,000×g for 70 min again and stored at –80°C.

Loading of Rifampin by Electroporation

200 µg exosomes and 200 µg RIF were mixed in an electroporation cuvette with PBS to a final volume of 500 µL.¹⁹ The entire process was conducted in an ice bath. Then, the mixture was electroporated under the following conditions: 500 V, discharged once for 1 ms. After electroporation, the suspension was incubated at 4°C for 15 min and then at 37°C for 1 h to facilitate drug diffusion and pore closure. Finally, the mixture was centrifuged at 4000×g for 30 min twice in 100 KDa ultrafiltration tubes to remove extra-exosomal RIF. Subsequently, nanoparticle tracking analysis (NTA), transmission electron microscopy (TEM) and Western blot (WB) detection of the exosomes were performed.

Identification and Quantification of RIF Loaded in Exosomes

After drug loading by electroporation, we verified that RIF was successfully loaded in exosomes. First, the absorbance of RIF was measured at 473 nm with a spectrophotometer to generate the standard curve of the “absorbance value-concentration”. Then the absorbance values of the exosomes and Exo-RIF at 473 nm were measured, and the encapsulation efficiency was calculated.³⁰

Conjugation of the ANG-Peptide to the Exo-RIF

According to the research of Robert et al,³¹ we functionalized exosomes with sulfhydryl groups on the surface of exosomes. Exo-RIF were incubated with 200 µg of maleimide group-coupled ANG and stirred for 12 h at room temperature in the dark. During

this process, sulfhydryl groups conjugated with maleimide functional groups through thioether linkages. After the reaction, the unbound ANG was removed by ultrafiltration twice at $4000\times g$ for 30 min. Furthermore, NTA, TEM, and WB detection were performed on the engineered exosomes, and the results were compared with those obtained with free exosomes.

Verification and Quantification of the ANG-Peptide Conjugated on the Exosomes

The following experiments were performed to confirm the successful binding of ANG to the exosome surface: (1) The ANG-Exo-RIF was incubated on Exoview (Nanoview Biosciences, Brighton, MA) chips that coated with antibodies against CD9. Then the chips were imaged by scanner. (2) Exos in ANG-Exo-RIF were pre-labeled by DiI and then incubated with bend.3 cells in 12-well plate ($50\ \mu\text{g}$ exosomes and 1×10^5 cells per well). Then, two fluorescence signals (DiI and FITC conjugated to ANG) were observed under a fluorescence microscope. The ANG peptides were quantified using the following methods: (1) The absorbance of ANG (FITC) was measured at 490 nm with a spectrophotometer to draw the standard curve of “the absorbance value-concentration” of ANG. (2) After sample ultrafiltration, the supernatant was collected, and the absorbance value was measured at 490 nm to ascertain the content of ANG. The coupling efficiency was calculated as (total amount of ANG–amount of uncoupled ANG)/total amount of ANG. Furthermore, the surface density of ANG on the exosomes was calculated on the basis of the exosome particle concentration determined by NTA.²²

Biosafety of the ANG-Exo-RIF in vitro and in vivo

The biosafety of the ANG-Exo-RIF in vitro and in vivo was evaluated. Bend.3 cells were treated with RIF, Exo-RIF and ANG-Exo-RIF (with RIF concentrations of 0.25, 2.5, 5, 10 and 20 $\mu\text{g}/\text{mL}$) for 24 h, and then cell-counting-kit-8 (CCK-8) assays were performed. To evaluate the biosafety in vivo, twelve healthy C57BL/6 mice were randomly allocated 4 groups as follows: (1) PBS; (2) ANG-Exo-RIF; (3) ANG-Exo-RIF; (4) RIF. The dose of RIF was 10 mg/kg. Different agents were injected into the mice respectively. Thirty days after administration, the mice were sacrificed to collect serum for biochemical examination and various organs were isolated for histological analyses.

The Targeting Efficiency of ANG-Exo-RIF in vitro

In order to evaluate the targeting ability of ANG-Exo-RIF in vitro, exosome was pre-labeled by DiI. The experiment was divided into four groups: (1) ANG-Exo-RIF + bend.3 (2) Exo-RIF + bend.3 (3) ANG-Exo-RIF + bend.3 (pre-blocked by free ANG peptide, 100 $\mu\text{g}/\text{mL}$, 0.5 h) (4) ANG-Exo-RIF + astrocyte. The cells (1×10^5) were seeded into 12-well plate and co-incubated with different samples for 4 h at 37°C. After the end of incubation, fluorescence intensity of each group was observed by fluorescent microscopy and quantified by flow cytometry.

Establishment of Vitro BBB Model

For establishment of BBB model, a previously reported method was used.³² Briefly, 5×10^4 bend.3 cells were seed on the front side of transwell chamber (0.4 μm) in 24-well plates. The low chamber was filled with complete medium. The culture medium was updated for every 2 days. The trans-endothelial electrical resistance (TEER) was measured daily to monitor the integrity of cell monolayer and sodium fluorescein were used to evaluate the permeability of BBB model.

Verification That ANG-Exo-RIF Cross the Blood Brain Barrier Model in vitro

For transcytosis study, Exo-RIF, ANG-Exo-RIF and RIF (RIF concentration: 250 $\mu\text{g}/\text{mL}$) were added to the upper chamber of a transwell respectively. As for the blocked group, the BBB model was pre-treated with free ANG-peptide (100 $\mu\text{g}/\text{mL}$) for 0.5 h before adding ANG-Exo-RIF in vitro. The aliquots were collected from the lower chamber at 24 h and absorbance value was determined at 334 nm. The transportation ratio (%) = amount of RIF in the basolateral compartment/initial amount.²²

The Targeting Efficiency of ANG-Exo-RIF in vivo

To evaluate the targeting efficiency of ANG-EXO-RIF in vivo, exosomes were labeled with DiI for tracing. C57BL/6 mice were allocated to different groups (n = 3): (1) Targeted group: ANG-Exo-RIF and (2) Nontargeted group: Exo-RIF. Each reagent was injected into the tail vein (200 μg Exosomes/200 μL PBS). The biological distribution of the ANG-Exo-RIF

in vivo was then evaluated using near-infrared fluorescence imaging at 1 h, 2 h, 4 h, 8 h, 12 h, 24 h, 48 h and 72 h after injection. Then, the mice were sacrificed and brain tissue sections were frozen and then observed under fluorescence microscopy.

In order to further study the real situation of drugs in the brain, Cy7 conjugated RIF was used (purchased from Xi'an ruixi Biological Technology Co., Ltd, Xian, China). Twelve C57BL/6 mice were divided into three group with three mice in each group: (1) RIF (2) Exo-RIF (3) ANG-Exo-RIF. Each reagent was injected into the tail vein (RIF concentration of 1mg/mL) and then near-infrared fluorescence imaging was performed at 1 h, 2 h, 4 h, 8 h, 24 h after injection. In addition, organs were harvested for ex vivo fluorescence imaging at 1 h, 12 h, 24 h after injection.

In vitro Antibacterial Activity of the RIF Loaded in the Exosomes

The MIC and minimum bactericidal concentration (MBC) of drugs are important indicators of antibacterial activity. An experiment was established with four groups: (1) RIF group, (2) Exo-RIF group, (3) ANG-Exo-RIF group and (4) Exo group. The MIC for the H37Rv strain was determined through microplate alamar blue assay (MABA). Then, 100 μ L 7h9 medium and 100 μ L H37Rv strain (mcf = 0.05) were added to 96-well plates. The concentrations (0.0625, 0.125, 0.25, 0.5, 1, 2, 4, 8 and 16 μ g/mL) of RIF in each group were identical in each group, and RIF solution was added to columns 1–10, respectively. In the Exo group, the concentration of the exosomes was the same as that in the other groups. Column 11 (without the drugs) was used as the control, and column 12 (without drugs with the H37Rv strain) was used as the blank group. The plates were incubated for 2 weeks, and 5 μ L of the supernatant was taken from columns 1–11 and added to the 7H10 solid medium and then incubated for 24 hours. The MBC is recognized as the lowest concentration at which no colony grew. Alamar blue agent was added to the contents of the 96-well plates, which were and re-incubated for 24 h. Blue indicated no colony growth, and pink indicated colony growth.³³

Statistical Analysis

The data are shown as the means \pm standard deviation (SD) of at least three independent experiments and were analyzed using GraphPad Prism version 7.0 software (GraphPad Software, Inc., San Diego, CA, USA). The differences in two groups were compared by Student's *t*-test. The differences between the two groups were considered statistically significant when **P* < 0.05, and very significant when ***P* < 0.01 or ****P* < 0.001.

Results

Characterization of Primary BMSCs

Exosomes, as promising carriers for drug delivery, need to be selected based on an appropriate cell source. We selected MSCs as the parent cells because of their high exosome production efficiency and biosafety.³⁴ The cells from bone marrow samples were incubated for 48 h, and then, unattached cells were washed away. Under a microscope, single cells showed a typical polygonal, spindle-like, fibroblast-like morphology. From day 2 to day 4, the cells grew slowly and then grew rapidly in a whirlpool-like arrangement. The 5th generation of cells retained a consistent morphology (Figure S1a). Furthermore, the surface markers of the 3rd-generation cell were analyzed by flow cytometry. The results showed that the cells were positive for the specific markers CD44 (98.2%) and SCA-1 (68%), and were negative for CD11B (1.94%), CD31 (6.85%) and CD45 (7.26%) expression (Figure S1b). The cells produced lipid droplets (Figure S1c-1) and calcium nodules (Figure S1c-2) after induced differentiation, indicating that the cells exhibited multipotential differentiation. These data indicated that the cells were BMSCs. BMSCs in passages 2 through 8 (P2-P8) were cultured to produce exosomes.

Isolation and Characterization of the Exosomes

Exosomes were isolated from the culture medium of BMSCs by differential ultracentrifugation and concentrated to 1 mL of exosomes per 1000 mL of supernatant. The exosomes were negatively stained with uranyl acetate and observed by TEM. The TEM images showed that the exosomes were round and cup-shaped vesicles with a double-layer membrane structure. The exosome diameter was approximately 50–150 nm (Figure 1A-1). These characteristics were consistent with exosomes

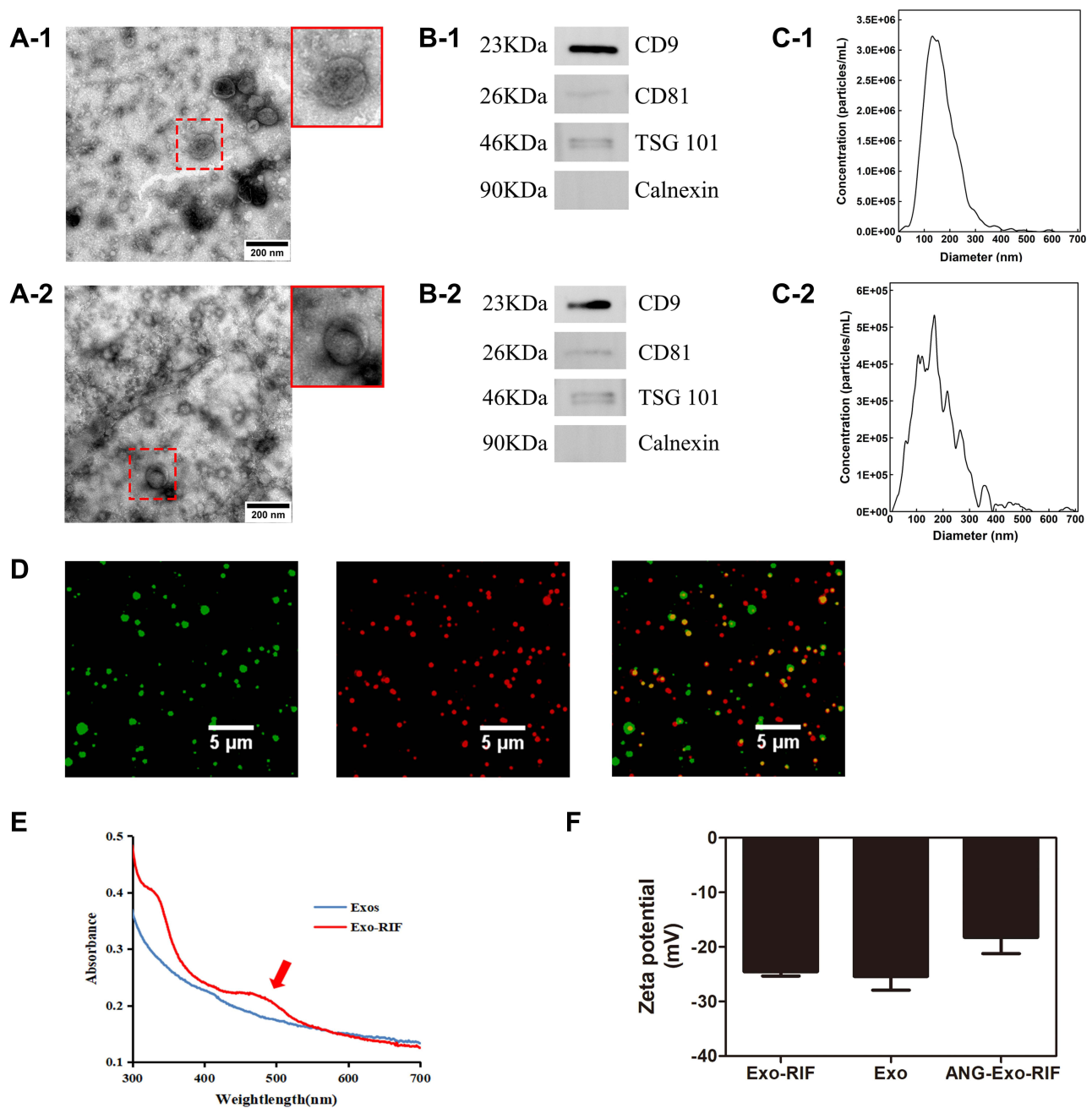


Figure 1 Characterization of the Exo and ANG-Exo-RIF. TEM image of free Exos (**A-1**) and ANG-Exo-RIF (**A-2**). Characteristic membrane protein of Exos (**B-1**) and ANG-Exo-RIF (**B-2**) analyzed by Western blot. Size distribution of Exos (**C-1**) and ANG-Exo-RIF (**C-2**) examined by NTA. (**D**) ANG-Exo-RIF observed by Exoview. The green fluorescence represents ANG (labeled with FITC), and the red fluorescence represents Exos (labeled with anti-CD81-Alexa 555). Merged fluorescence is shown in yellow indicated colocalization. (**E**) UV-Vis absorption spectrum of Exo (blue line) and Exo-RIF (red line), Exo-RIF has absorption peak at 473nm (red arrow). (**F**) The zeta potential of Exo, Exo-RIF and ANG-Exo-RIF.

according to reported previously.³⁵ WB showed expression of the positive exosome markers CD9, CD81 and TSG101 and the absence of the negative marker calnexin in isolated samples (**Figure 1B-1**). An NTA showed that the concentration of the exosomes was $1.8 \pm 2.3 \times 10^{11}$ particles/mL, and the size distribution peak was 156.7 ± 4.1 nm (**Figure 1C-1**). The zeta potential of the exosomes was -25.39 ± 2.53 mV, which meant that exosomes were very stable and would not aggregate in solution.³⁶ The protein concentration of the exosomes was determined by bicinchoninic acid assay (BCA) and was 2.53 ± 0.39 mg/mL. In summary, all these data indicated that the exosomes had been successfully isolated and that the concentration was sufficient for use in subsequent experiments.

Characterization of the ANG-Exo-RIF

After electroporation, Exo-RIF was obtained. As shown in [Figure 1F](#), the zeta potential of the Exo-RIF was -24.53 ± 0.79 mV, which was negligibly different than change that of the Exos, suggesting that RIF successfully loaded in the exosomes did not change the surface properties of the exosomes. Subsequently, Exo-RIF were modified with ANG, and ANG-Exo-RIF were obtained. The zeta potential of ANG-Exo-RIF was -18.21 ± 2.99 mV with a slight increase, which may have been related to the peptide modified on the member. To determine whether the engineered exosomes remain intact, a series of experiments were performed. First, TEM showed that ANG-Exo-RIF maintain an intact membrane structure without any changes ([Figure 1A–2](#)). Second, the relative expression of the exosome markers CD9, CD8 and TSG101 remained positive, and that of calnexin remained negative ([Figure 1B–2](#)). Third, an NTA indicated a peak value of 165.9 ± 3.5 nm, which represented a slight increase compared with that in the Exos ([Figure 1C–2](#)). However, this change was within a reasonable range, which can be interpreted as a result of drug loading and peptide linking. These data demonstrated that ANG-Exo-RIF maintained the integrity and properties of unloaded and unmodified exosomes.

Verification and Quantification of the ANG Peptide on the Exosomes

To confirm that ANG had been successfully conjugated to the surface of exosomes, the prepared ANG-Exo-RIF was observed by Exoview R200 (Nanoview Biosciences, Brighton, MA). Exosomes labeled with anti-CD9 appeared red, and ANG labeled with FITC appeared green. We found that the green and red signals displayed extensive colocalization ([Figure 1D](#)). In addition, we also labeled Exos in ANG-Exo-RIF with DiI and then co-incubated with bend.3 cells for 2h. The fluorescence microscope image ([Figure S2](#)) also showed the extensive colocalization of Exos (labeled with DiI, red) and ANG (labeled with FITC, green), which meant that ANG had been successfully linked to the exosomes ([Figure 1D](#)). Then, the relative quantification of ANG was determined. The coupling efficiency was calculated by dividing the amount of ANG on the surface of the exosomes by the total amount of added ANG. After calculation, the standard curve of ANG was $y = 7.0426x + 0.3628$ and the coupling efficiency was $15.8 \pm 2.4\%$. According to the number of particles determined by NTA, $9.2 \pm 1.5 \times 10^4$ ANG peptides were attached to each exosome.

Identification and Quantification of RIF Loading in the Exosomes

RIF was loaded into exosomes by electroporation, and the RIF-loaded exosomes were purified by ultrafiltration. To verify that RIF had been successfully loaded into exosomes, ultraviolet-visible (UV-vis) spectroscopy was performed. After purification, the retained Exo-RIF was scanned by the fully UV-vis wavelength spectrum. The results showed that the retained Exo-RIF had a characteristic peak at 473 nm, which was the peak characteristic of RIF, suggesting that RIF had been successfully loaded ([Figure 1E](#)). According to the standard curve, the encapsulation efficiency was $18.8 \pm 2.4\%$, and the concentration of RIF was 37.6 ± 4.8 μ g per 200 μ g of exosomes.

Biosafety of ANG-Exo-RIF in vitro and in vivo

As shown in [Figure 2](#), CCK-8 assays showed that the viability of the bend.3 cells treated with ANG-Exo-RIF, Exo-RIF or RIF has all reached 80%, indicating that ANG-Exo-RIF induced little toxicity to cells. Then, we evaluated the toxicity induced by ANG-Exo-RIF in vivo. Aspartate aminotransferase (AST), creatine kinase (CK) and serum creatinine (Scr) levels were measured to determine the function of the heart, liver, and kidney in the treated mice. The results showed all the indexes in each group were within the normal reference ranges ([Table S1](#)). Furthermore, hematoxylin-eosin (HE) staining of various organs revealed no pathological changes in any group ([Figure 2](#)). These results indicated that ANG-Exo-RIF were safe biomaterials for in vivo application.

The Targeting Ability of ANG-Exo-RIF in vitro

Brain microvascular endothelial cells exhibit high expression of LRP1, which is expressed at low levels in astrocyte cells.²² Therefore, we chose bend.3 cells as target cells and astrocytes as nontarget cells. We extracted primary astrocytes from Sprague–Dawley (SD) rats, and the purity of astrocytes was determined by GFAP staining. As presented in [Figure S3a](#),

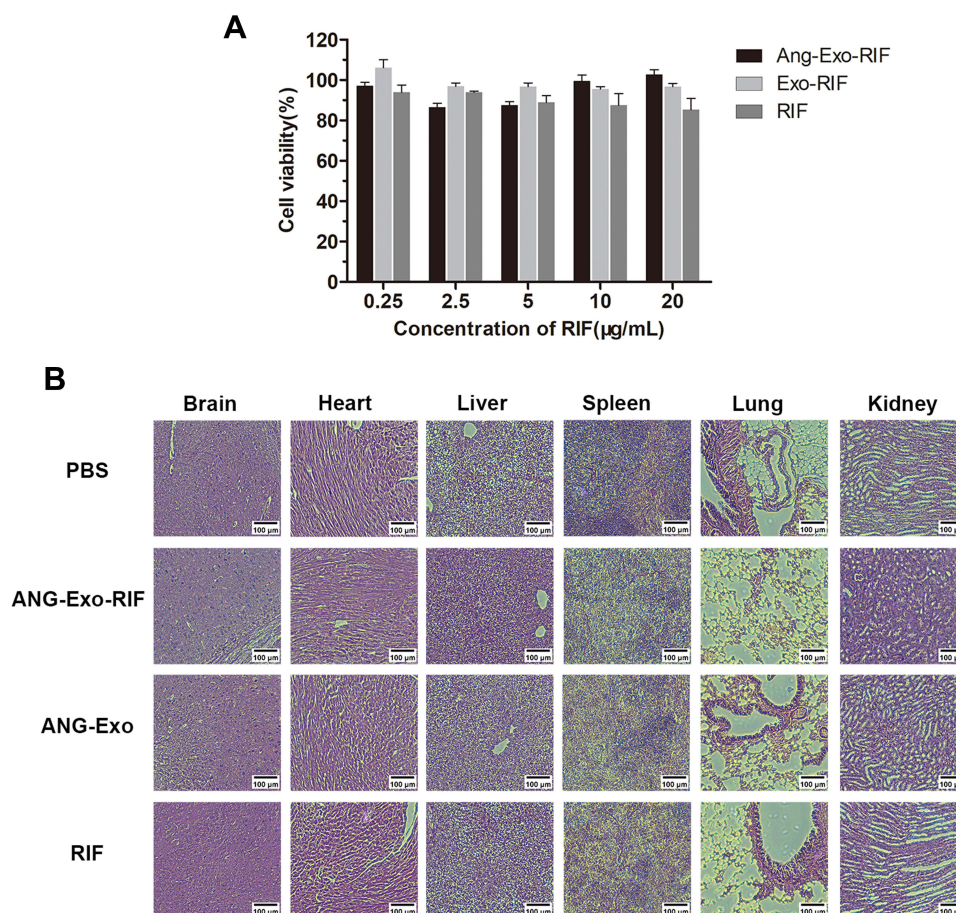


Figure 2 Biosafety of ANG-Exo-RIF in vitro and in vivo. **(A)** Bend.3 cells were treated with RIF, Exo-RIF and ANG-Exo-RIF for 24h, then the cell viability was detected by CCK8 assays. **(B)** HE staining analysis of main organs in mice 30 days after intravenous injection of different agents.

GFAP-immunolabeled astrocytes are shown in green. The purity of the astrocytes assessed by flow cytometry and was found to have reached 97.5% (Figure S3b). Then, the following experiment was performed.

DiI-labeled exosomes were incubated with bend.3 cells or astrocyte cells for 4 h, and then the fluorescence intensity was then observed (Figure 3A). The strongest fluorescence intensity was shown in the bend.3 cells incubated with ANG-Exo-RIF, and this intensity was significantly higher than that of bend.3 cells incubated with Exo-RIF. However, the intensity was significantly weakened when bend.3 cells were pre-blocked with the ANG peptide before incubation with ANG-Exo-RIF. The group of astrocyte cells incubated with ANG-Exo-RIF exhibited the same fluorescence intensity as the non-targeted group and pre-blocked group. Therefore, we concluded that ANG-Exo-RIF can specifically target bend.3 cells and that this targeting ability was due to the binding of the ANG peptide to LRP1. To verify the targeting ability of ANG-Exo-RIF, flow cytometry was performed and the mean fluorescence intensity (MFI) of cells was semi-quantitated. The highest MFI was observed in the “ANG-Exo-RIF + bend.3” group and was more than three-fold higher than that of the other groups (Figures 3B and S4).

The Ability of ANG-Exo-RIF Cross the BBB in vitro

As shown in Figure 4A, bend.3 cell monolayers were cultured in Transwell chambers to mimic the BBB in vitro. The TEER value of the BBB model was $230.6 \pm 6.6 \Omega \times \text{cm}^2$ on day 7 after cell seeding, and the permeability coefficient was $1.6 \pm 0.5 \times 10^{-3} \text{cm/min}$, which is similar to literature reported before, indicating the BBB model has been successfully established in vitro.³⁷

The transport ratio of the ANG-Exo-RIF was $52.11 \pm 5.68\%$, which was two-fold higher than nontargeted Exo-RIF ($23.82 \pm 3.18\%$). Moreover, the transport ratio of the ANG-Exo-RIF ($13.9 \pm 3.39\%$) was significantly decreased by

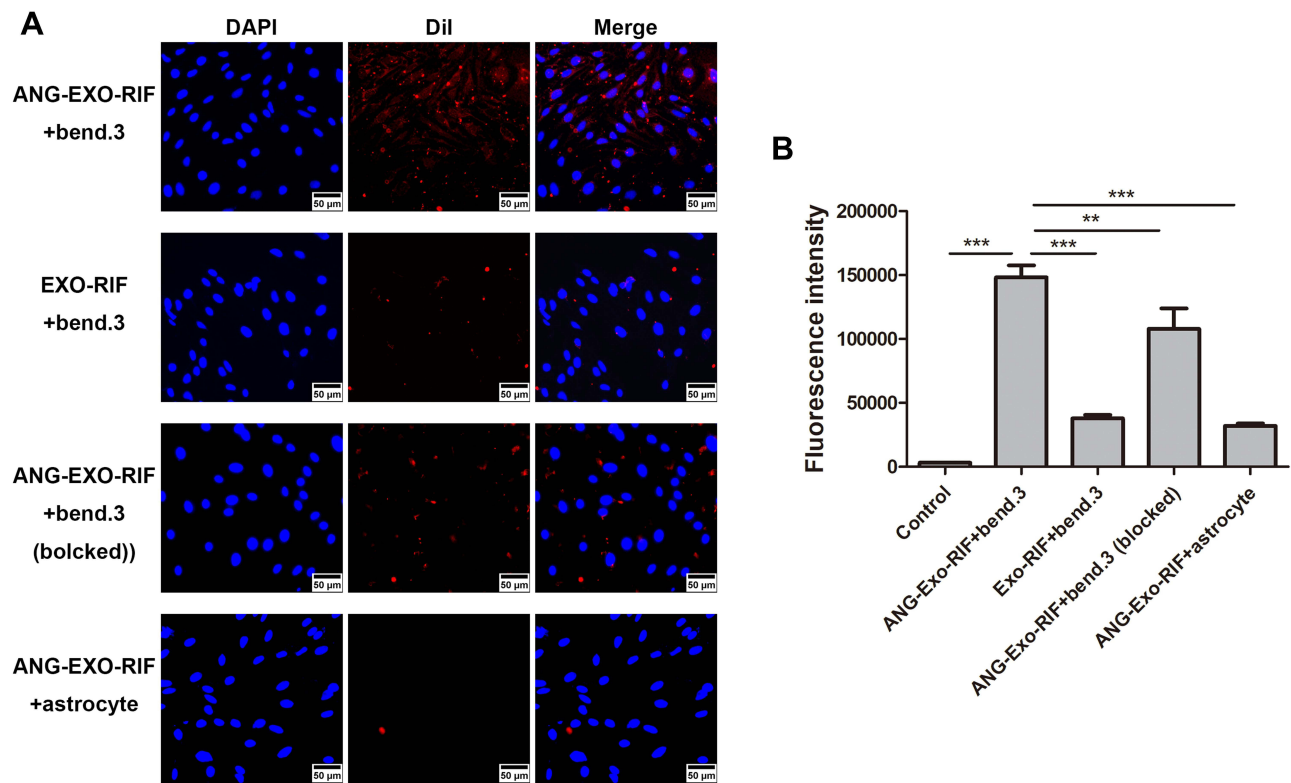


Figure 3 The targeting capability of ANG-Exo-RIF in vitro. **(A)** Bend.3 cells and astrocyte cells were treated with ANG-Exo-RIF and Exo-RIF. Blue: nucleus stained by DAPI. Red: exosomes dyed by DiI. **(B)** Mean fluorescence intensities of different groups according to flow cytometric results, each bar represents the mean \pm SD of three replicates. **Means $p < 0.01$, ***Means $p < 0.001$.

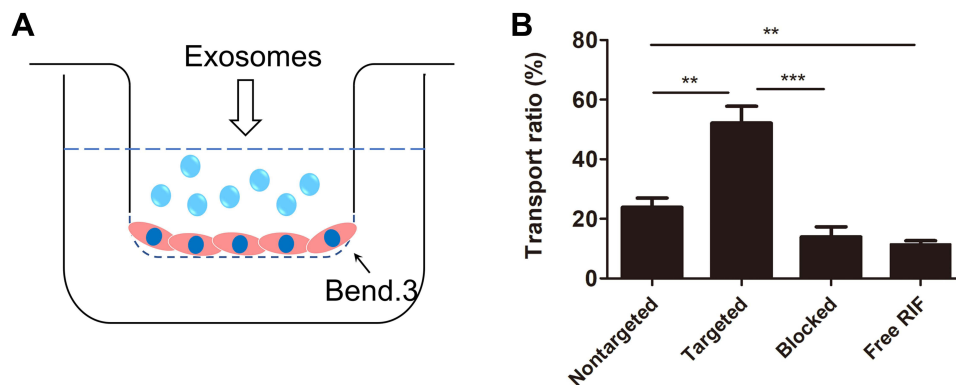


Figure 4 The ability of ANG-EXO-RIF cross the BBB in vitro. **(A)** Illustration of Exos crossing the BBB model established by monolayers of Bend.3 cells. **(B)** The in vitro BBB model transport ratio (%) of ANG-Exo-RIF and Exo-RIF following 24h incubation. Each bar represents the mean \pm SD of three replicates. **Means $p < 0.01$, ***Means $p < 0.001$.

pretreating the in vitro BBB model with free ANG peptide, indicating the surface modification can assist more exosomes cross the BBB. In addition, the transport ratio of free RIF was $11.4 \pm 1.25\%$, lower than that of Exo-RIF, proving that exosome encapsulation can improve the BBB permeability of drugs (Figure 4B). These results demonstrated the exosome-loading and modification were effective.

The Targeting Ability of ANG-Exo-RIF in vivo

Based on the aforementioned targeting experimental results, fluorescence imaging was performed to detect the targeting ability of the ANG-Exo-RIF in vivo. DiI labeled ANG-Exo-RIF (referred to as targeted group) and Exo-RIF (referred to

as non-targeted group) were injected into C57BL/6 mice through the tail vein. Then the distribution and intensity of the fluorescence were recorded at 1 h, 2 h, 4 h, 8 h, 12 h, 24 h, 48 h and 72 h. Furthermore, the fluorescence intensity of the brain region was measured. As shown in Figure 5A and C, the targeted group showed a higher fluorescence intensity in the brain region than the non-targeted group from the first hour. The strongest fluorescence intensity of non-targeted group was achieved at the 24 h time point and had decreased by the following time point. In the targeted group, the fluorescence intensity of brain region kept increasing until 48h after injection. In the whole time point, the fluorescence signal of brain in targeted group was always higher than that in non-targeted group. To more fully observing the distribution of exosomes in two groups, the organs were isolated and observed at 24 h after injection (the time point that untargeted group had strongest fluorescence intensity). The fluorescence intensity of ex vivo brain in targeted group than in non-targeted group (Figure 5B). As expected, unmodified exosomes would prefer to accumulate in liver (Figure S5). In addition to liver, little fluorescence could also be observed in other organs. Then, brains were frozen, sectioned and observed. As Figure 5D shown, the red fluorescence near the cell nucleus in the frozen brain tissue slices was exosome. Exosomes could be observed in the cortex, and more exosomes could be observed in the targeted group than in the non-targeted group. These results suggested that the modification of ANG can endow exosomes with excellent targeting ability to brain.

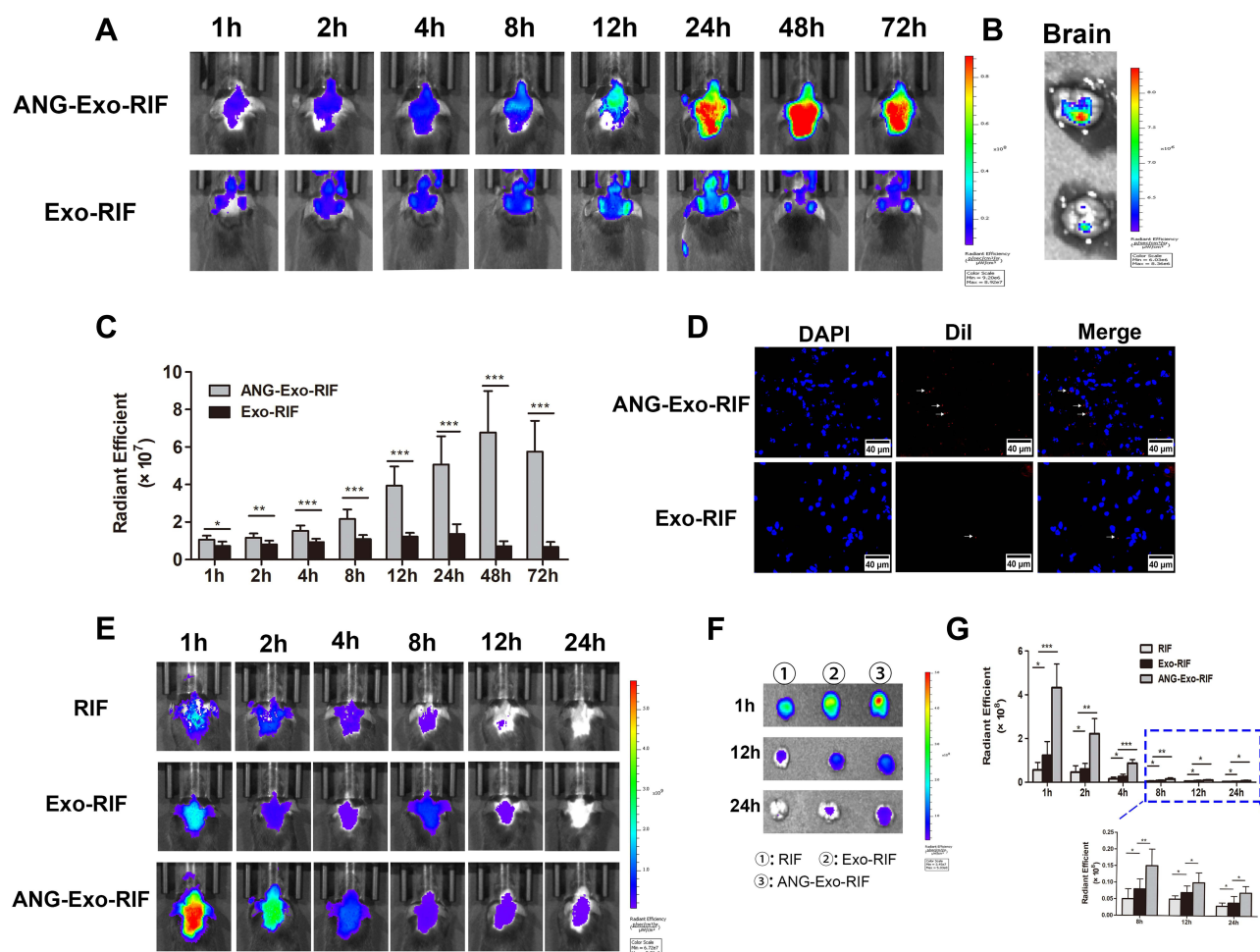


Figure 5 The targeting capability of ANG-Exo-RIF in vivo. **(A)** In vivo fluorescence images of ANG-Exo-RIF and Exo-RIF in mice (fluorescence represents Dil-labeled exosomes). **(B)** Ex vivo fluorescence images of isolated brains at 24h after intravenous administration of Dil-labeled exosomes. **(C)** Comparison of the radiant efficiencies of Dil-labeled exosome in brain region between ANG-Exo-RIF and Exo-RIF groups at the different time points. **(D)** Frozen section of brain tissue in targeted group and non-targeted group. Red: exosomes labeled with Dil (white arrow). Blue: nuclei stained with DAPI. **(E)** In vivo fluorescence images of mice in different groups (fluorescence represents Cy7-RIF). **(F)** Ex vivo fluorescence images of isolated brain at 1h, 12h, 24h after administration (fluorescence represents Cy7-RIF). **(G)** The radiant efficiencies of Cy7-RIF in brain region of different groups at different time points. Each bar represents the mean \pm SD of three replicates. *Means $P < 0.05$, **Means $P < 0.01$, and ***Means $P < 0.001$.

Table 1 MIC and MBC of Rifampicin-Loaded Exosomes Against H37Rv

	MIC ($\mu\text{g/mL}$)	MBC ($\mu\text{g/mL}$)
ANG-Exo-RIF	0.25	0.25
Exo-RIF	0.25	0.25
RIF	0.25	0.25
Exo	>100	>100

We further investigated the real situation of drugs in the brain by using Cy7 conjugated RIF. As shown in [Figure 5E and G](#), the fluorescence intensity of ANG-Exo-RIF group was the highest, followed by Exo-RIF group and the fluorescence intensity of RIF group was the lowest. The fluorescence intensity of all three groups reached peak at 1 h after injection and began to decline subsequently. In ex vivo brain images ([Figure 5F](#)), ANG-Exo-RIF group showed strongest fluorescence. As we expected, exosomes can help drugs cross the BBB, but cannot actively target to the brain. Exosomes can accumulate in the brain after targeted modification, which is consistent with the transwell assay in vitro. In addition, we also collected other organs, such as heart, liver, spleen, lung, kidney of mice and investigated distribution of RIF in each organ. As shown in [Figure S6](#), strong fluorescence could be observed in liver and spleen because of their scavenging and metabolic functions. As time go on, the whole fluorescence decreased. Taken together, these results demonstrated that ANG-Exo-RIF can efficiently targeted the brain, which provided a good basis for future studies.

In vitro Antibacterial Activity of RIF Loaded in the Exosomes

MIC and MBC were determined, and the results showed that RIF, Exo-RIF and ANG-Exo-RIF demonstrated MIC and MBC of 0.25 $\mu\text{g/mL}$ against H37Rv strain, indicating that the exosomes encapsulating did not influence the antibacterial properties of RIF ([Table 1](#)). In addition, the result showed that free exosomes had no antibacterial activity.

Discussion

CNS-TB is the most severe type of TB, causing high morbidity and mortality.³⁸ As one of the most important anti-tuberculosis drugs, RIF plays a key role in treatment. However, the low BBB permeability of RIF greatly limits its therapeutic effect and remains a challenge for treatment of CNS-TB. Drug delivery systems are widely used and studied due to their high efficiency on drug delivery. Hence, searching for an appropriate drug carrier may be a feasible strategy for treating CNS-TB. In the present study, artificial synthetic carriers, such as liposomes, upconverting nanoparticles, and polymer vesicles, show some drawbacks, including high toxicity and immunogenicity.^{39,40} Exosomes, as natural carriers derived from cells, display significant advantages in drug delivery compared with traditional drug carriers. Remarkably, exosomes can overcome the BBB because of their cell-like properties.⁴¹ Hence, we chose exosomes as RIF carriers. However, unmodified exosomes lack targeting ability, which limits the enrichment of exosomes in the brain. Several studies have revealed that Angiopep-2 is the most advanced BBB shuttle peptide being tested in current clinical trials and can increase the concentration of drugs in the brain.⁴² Therefore, we chemically modified the surface of exosomes with ANG to achieve targeted delivery. Ultimately, a targeted drug system named ANG-Exo-RIF was designed.

In this study, we first successfully extracted primary BMSCs and obtained sufficient supernatant, which provided a basis for the successful acquisition of exosomes. Then, the related characterization of exosomes and ANG-Exo-RIF were conducted and compared. Additionally, the concentration of ANG on the exosomes and RIF levels in the exosomes were quantified. The results showed that the characteristics of the engineered exosomes were not altered by these modifications and were similar to those of free exosomes. Moreover, the ANG-Exo-RIF showed good coupling and encapsulation efficiency, indicating that we had successfully constructed ANG-Exo-RIF nanoparticles.

Then, we further evaluated the targeting ability of ANG-Exo-RIF in vitro and in vivo. Using fluorescence microscopy, we found that ANG-Exo-RIF were easily taken up by brain microvessel endothelial cells, which also had been proven by flow cytometry analysis. Furthermore, we constructed an in vitro BBB model and tested the transport of ANG-Exo-RIF. The results showed that Exo-RIF had better ability to penetrate BBB compared with free RIF and ANG peptide facilitated the movement of more exosomes across the BBB in vitro. These results indicated that ANG-Exo-RIF showed

good targeting ability and BBB penetration capacity in vitro. Then, an in vivo targeting experiment was performed. Fluorescence imaging showed much more intense fluorescence in the brain tissue of the ANG-Exo-RIF group compared with that in the Exo-RIF group, which indicated the excellent targeting ability of ANG-Exo-RIF to the BBB. Moreover, the results showed that free exosomes also crossed the BBB, which was consistent with literature reports.⁴³ However, the mechanisms are still not clear and multiple mechanisms may be involved.⁴⁴

MIC and MBC are generally used to evaluate the effects of antibacterial agents. We found that the antituberculosis activity of exosome-loaded RIF was not altered upon loading into exosomes and that it was similar to that of free RIF, which can lay the foundation for treatment in future. Notably, MIC and MBC indicate extracellular antibacterial activity. However, *Mycobacterium tuberculosis* is an intracellular bacterium. Yang et al found that exosomes as carriers of antibacterial drugs can deliver drugs into cells and improve intracellular antibacterial activity.⁴⁵ Thus, RIF in exosomes may produce the same effect in cells with internal infection. In addition, it has been reported that when endothelial cells are exposed to RIF for a long time, RIF upregulates the expression of P-gp, which is a specific active efflux transporter in the BBB.⁴⁶ So, RIF stealthily delivered in exosomes may pass the BBB more smoothly than RIF in free applications. Therefore, we believe that RIF encapsulated in exosomes shows future clinical translation potential.

Nevertheless, we also found some unexpected results. In vivo targeting experiments, we explored the targeting ability of ANG-Exo-RIF in different labeling methods, one is the labeling exosomes (DiI-Exo), which is widely used in current research, and the other is labeling RIF (Cy7-RIF). Both methods confirmed that ANG-Exo-RIF has excellent targeting ability, but the time points of peak fluorescence intensity were different. The fluorescence intensity of DiI-Exo could keep rising for long time until 48h after injection, but the fluorescence intensity of Cy7-RIF reached peak at 1h after injection and decline subsequently. This discrepancy may be due to the properties of exosomes, high biocompatibility, and cell membrane like structure, allowing exosomes to be internalized by cells and release drugs easily. It also suggests that the behavior of drug and carrier in vivo cannot be mixed up, and researchers should take this into account when designing experiments.

The present research on a drug delivery system for the treatment of TB is still remains in the choice of artificial synthetic carriers, such as liposomes and polymeric micelles. For CNS-TB, Marcanes et al⁷ developed a gatifloxacin-loaded PLGA delivery system; Castro et al³⁸ encapsulated clofazimine with PLGA-PEG nanoparticles. However, these carriers have shown some clear drawbacks, including immune rejection, biocompatibility, and poor cell adhesion. Comparing with artificial carriers, exosomes can avoid toxicity caused by chemical reagent. In addition, exosomes have biological activity that artificial carriers do not have. For instance, exosomes derived from MSC have anti-inflammatory and regenerative ability, which may be an adjunct to treatment.⁴⁷ Moreover, *Mycobacterium tuberculosis* is an intracellular bacterium, encapsulating drug into exosomes may be more easily internalized by cells than into artificial carrier. Therefore, exosomes are a promising carrier in treatment of TB. However, there are few literatures reported exosomes as drug carrier for TB treatment. We innovatively developed an anti-TB drug loaded exosomes and modified the exosomes via simple methods to target the BBB, which achieved good results. This novel exosome-based nano-drug delivery system provided a new direction for future research.

However, this study has some shortcomings. Regarding antibacterial activity, we determine only the MIC and MBC of the ANG-Exo-RIF and did not perform treatment experiments in vivo due to the limitations of the laboratory conditions. In the future, we will further explore the intracellular antibacterial activity and treatment effect of ANG-Exo-RIF in vivo. In addition, to achieve clinical translation, we need to optimize certain details of the delivery system, such as improving the encapsulation efficiency and finding the most appropriate density of the peptide to determine the best combination of between cells and exosomes. Furthermore, we will compare drug delivery with exosomes and with artificial drug carriers (such as liposomes) from multiple perspectives, such as the encapsulation efficiency, BBB permeability with or without the peptide, and biosafety, to confirm the advantages of using exosome delivery systems. Clinically, CNS-TB patients usually need to be treated with multiple drugs, and exosomes have the ability to encapsulate multiple drugs.⁴⁸ We can explore the optimal doses and drug combinations to achieve the best treatments. In addition, despite current research shows that exosome is a promising carrier. However, there are some questions cannot be ignored when it comes to clinical application. Firstly, the primary challenge of obtaining exosomes is how to isolate and purify exosomes efficiently. Among existing exosome separation technologies, differential ultracentrifugation and density gradient centrifugation are two of the most common methods. However, the technologies we mentioned above may

cause exosomes rupture and aggregation.⁴⁹ The equipment used in ultrafiltration centrifugation is low-cost, but this method is easy to cause aggregation and yield loss.⁵⁰ The high purity of exosomes can be obtained by size exclusion chromatography, with disadvantage of time-consuming and unscalable.⁵¹ So, this method is not suitable to be applied to industrial production. In a word, it is urgent to develop an efficient and economical method to standardize the production high purity exosomes. Secondly, the drug-loading capacity limits clinical translation of exosome-based nanocarrier. This may attribute to the presence of phospholipids, which protect exosomes from degradation, and the presence of parental cell contents, which limit the confined space for exogenous drug loading.⁵² Thirdly, the unmodified exosomes lack of targeting ability and tend to accumulate in the liver, resulting in inefficient drug delivery. Thus, modification, including genetic engineering and chemical modification, is an effective method to enhance exosome targeting ability.¹² Genetic engineering is limited of complex operation, small selection range, and parent cell dependent transfection efficiency. In contrast, chemical modification is more flexible.⁵³ However, chemical modification should be performed after exosome isolation, which may disrupt membrane integrity. Except for modification, it is also a promising strategy to take advantage of exosome heterogeneity to select exosomes from different kinds of cells as nanocarriers. Exosome derived from different cells possess different biological characteristics *in vivo*. Wen et al⁵⁴ found that lung fibroblast cell derived exosomes can accumulate in lung. In addition, natural killer cell derived exosomes can target to tumor through homing effect.⁵⁵ However, this heterogeneity may also be an obstacle to the industrialization of exosomes. All in all, only after continuous exploration, comparison and optimization can make exosomes more capable of clinical application.

Conclusion

In summary, a new exosome-based, RIF-loaded, brain-targeting drug delivery system was fabricated for the treatment of CNS-TB and named ANG-Exo-RIF, which showed good biocompatibility. Our study demonstrated that ANG-Exo-RIF exhibited excellent brain targeting ability *in vitro* and *in vivo*, and the RIF antibacterial activity was not altered by exosome loading and modification and was comparable with that of free RIF. Thus, the use of ANG-Exo-RIF represents a promising strategy for the future translation of drug treatment for CNS-TB and other diseases in which permeating the BBB remains a challenge.

Abbreviation

CNS-TB, Central nervous system tuberculosis; RIF, Rifampin; BBB, Blood brain barrier; CSF, Cerebrospinal fluid; MIC, Minimum inhibitory concentration; RNA, Ribonucleic acid; LRP1, Low-density lipoprotein receptor-related protein 1; ANG, Angiotensin II type 2 receptor antagonist; MSCs, Mesenchymal stem cells; DMEM, Dulbecco's modified Eagle's medium; FBS, Fetal bovine serum; BMSCs, Bone marrow mesenchymal stem cells; PBS, Phosphate buffer saline; NTA, Nanoparticle tracking analysis; TEM, Transmission electron microscopy; TEER, Trans-endothelial electrical resistance; MBC, Minimum bactericidal concentration; SD, Standard deviations; WB, Western blot; UV-vis, Ultraviolet visible; MFI, Mean fluorescence intensity; CCK8, Cell-counting-kit-8; CK, Creatine kinase; AST, Aspartate aminotransferase; Scr, Serum creatinine; HE, Hematoxylin-eosin.

Data Sharing Statement

The datasets used and analyzed during the current study are available from the corresponding author on reasonable request.

Ethics Approval and Informed Consent

All animal procedures were performed according to the Institutional Animal Care & Use Committee at the The Second Hospital of Nanjing. Ethics approval number: 2018-LS-ky017.

Author Contributions

All authors made a significant contribution to the work reported, whether that is in the conception, study design, execution, acquisition of data, analysis and interpretation, or in all these areas; took part in drafting, revising or critically reviewing the article; gave final approval of the version to the published; have agreed on the journal to which the article has been submitted; and agree to be accountable for all aspects of the work.

Funding

We are grateful for the support by the Six talent peaks project in Jiangsu Province (WSN-160); the Key Project of Medical Science and Technology Development Foundation of Nanjing (ZKX18042); the Social Development Project of the Key Research and Development Plan of Jiangsu Province (BE2018606).

Disclosure

The authors have declared that no competing interest exists.

References

- Schaller MA, Wicke F, Foerch C, Weidauer S. Central nervous system tuberculosis: etiology, clinical manifestations and neuroradiological features. *Clin Neuroradiol*. 2019;29(1):3–18. doi:10.1007/s00062-018-0726-9
- Leonard JM. Central nervous system tuberculosis. *Microbiol Spectr*. 2017;5:2. doi:10.1128/microbiolspec.TNMI7-0044-2017
- Manyelo CM, Solomons RS, Walzl G, Chegou NN. Tuberculous meningitis: pathogenesis, immune responses, diagnostic challenges, and the potential of biomarker-based approaches. *J Clin Microbiol*. 2021;59:3. doi:10.1128/JCM.01771-20
- Ruiz-Bedoya CA, Mota F, Tucker EW, et al. High-dose rifampin improves bactericidal activity without increased intracerebral inflammation in animal models of tuberculous meningitis. *J Clin Invest*. 2022;132:6. doi:10.1172/JCI1155851
- Tucker EW, Guglieri-Lopez B, Ordonez AA, et al. Noninvasive (11) C-rifampin positron emission tomography reveals drug biodistribution in tuberculous meningitis. *Sci Transl Med*. 2018;10:470. doi:10.1126/scitranslmed.aau0965
- Savic RM, Ruslami R, Hibma JE, et al. Pediatric tuberculous meningitis: model-based approach to determining optimal doses of the anti-tuberculosis drugs rifampin and levofloxacin for children. *Clin Pharmacol Ther*. 2015;98(6):622–629. doi:10.1002/cpt.202
- Marcianes P, Negro S, Garcia-Garcia L, Montejó C, Barcia E, Fernandez-Carballido A. Surface-modified gatifloxacin nanoparticles with potential for treating central nervous system tuberculosis. *Int J Nanomedicine*. 2017;12:1959–1968. doi:10.2147/IJN.S130908
- Xie J, Shen Z, Anraku Y, Kataoka K, Chen X. Nanomaterial-based blood-brain-barrier (BBB) crossing strategies. *Biomaterials*. 2019;224:119491. doi:10.1016/j.biomaterials.2019.119491
- Luan X, Sansanaphongpricha K, Myers I, Chen H, Yuan H, Sun D. Engineering exosomes as refined biological nanoplatforams for drug delivery. *Acta Pharmacol Sin*. 2017;38(6):754–763. doi:10.1038/aps.2017.12
- Yang B, Chen Y, Shi J. Exosome biochemistry and advanced nanotechnology for next-generation theranostic platforms. *Adv Mater*. 2019;31(2):e1802896. doi:10.1002/adma.201802896
- Shao J, Zaro J, Shen Y. Advances in exosome-based drug delivery and tumor targeting: from tissue distribution to intracellular fate. *Int J Nanomedicine*. 2020;15:9355–9371. doi:10.2147/IJN.S281890
- Liang Y, Duan L, Lu J, Xia J. Engineering exosomes for targeted drug delivery. *Theranostics*. 2021;11(7):3183–3195. doi:10.7150/thno.52570
- Hu Y, Li X, Zhang Q, et al. Exosome-guided bone targeted delivery of Antagomir-188 as an anabolic therapy for bone loss. *Bioact Mater*. 2021;6(9):2905–2913. doi:10.1016/j.bioactmat.2021.02.014
- Ding Y, Wang L, Li H, et al. Application of lipid nanovesicle drug delivery system in cancer immunotherapy. *J Nanobiotechnology*. 2022;20(1):214. doi:10.1186/s12951-022-01429-2
- Mustapic M, Eitan E, Werner JK Jr, et al. Plasma extracellular vesicles enriched for neuronal origin: a potential window into brain pathologic processes. *Front Neurosci*. 2017;11:278. doi:10.3389/fnins.2017.00278
- Saint-Pol J, Gosselet F, Duban-Deweere S, Pottiez G, Karamanos Y. Targeting and crossing the blood-brain barrier with extracellular vesicles. *Cells*. 2020;9:4. doi:10.3390/cells9040851
- Wang J, Chen D, Ho EA. Challenges in the development and establishment of exosome-based drug delivery systems. *J Control Release*. 2021;329:894–906. doi:10.1016/j.jconrel.2020.10.020
- Tian T, Zhang HX, He CP, et al. Surface functionalized exosomes as targeted drug delivery vehicles for cerebral ischemia therapy. *Biomaterials*. 2018;150:137–149. doi:10.1016/j.biomaterials.2017.10.012
- Jia G, Han Y, An Y, et al. NRP-1 targeted and cargo-loaded exosomes facilitate simultaneous imaging and therapy of glioma in vitro and in vivo. *Biomaterials*. 2018;178:302–316. doi:10.1016/j.biomaterials.2018.06.029
- Zhu J, Zhang Y, Chen X, et al. Angiopep-2 modified lipid-coated mesoporous silica nanoparticles for glioma targeting therapy overcoming BBB. *Biochem Biophys Res Commun*. 2021;534:902–907. doi:10.1016/j.bbrc.2020.10.076
- Shi XX, Miao WM, Pang DW, et al. Angiopep-2 conjugated nanoparticles loaded with doxorubicin for the treatment of primary central nervous system lymphoma. *Biomater Sci*. 2020;8(5):1290–1297. doi:10.1039/C9BM01750J
- He C, Zhang Z, Ding Y, et al. LRP1-mediated pH-sensitive polymersomes facilitate combination therapy of glioblastoma in vitro and in vivo. *J Nanobiotechnology*. 2021;19(1):29. doi:10.1186/s12951-020-00751-x
- Xunian Z, Kalluri R. Biology and therapeutic potential of mesenchymal stem cell-derived exosomes. *Cancer Sci*. 2020;111(9):3100–3110. doi:10.1111/cas.14563
- Batrakova EV, Kim MS. Using exosomes, naturally-equipped nanocarriers, for drug delivery. *J Control Release*. 2015;219:396–405. doi:10.1016/j.jconrel.2015.07.030
- Phinney DG, Pittenger MF. Concise review: MSC-derived exosomes for cell-free therapy. *Stem Cells*. 2017;35(4):851–858. doi:10.1002/stem.2575
- Li XH, Zhang J, Li DF, Wu W, Xie ZW, Liu Q. Physiological and pathological insights into exosomes in the brain. *Zool Res*. 2020;41(4):365–372. doi:10.24272/j.issn.2095-8137.2020.043
- Cho CF, Wolfe JM, Fadzen CM, et al. Blood-brain-barrier spheroids as an in vitro screening platform for brain-penetrating agents. *Nat Commun*. 2017;8:15623. doi:10.1038/ncomms15623
- Hu L, Wang Y, Zhang Y, et al. Angiopep-2 modified PEGylated 2-methoxyestradiol micelles to treat the PC12 cells with oxygen-glucose deprivation/reoxygenation. *Colloids Surf B Biointerfaces*. 2018;171:638–646. doi:10.1016/j.colsurfb.2018.08.009

29. Revollo L, Kading J, Jeong SY, et al. N-cadherin Restrains PTH Activation of Lrp6/ β -catenin Signaling and Osteoanabolic Action. *J Bone Miner Res.* 2019;34(11):2163–2165. doi:10.1002/jbmr.3845
30. Ding Y, Yang R, Yu W, et al. Chitosan oligosaccharide decorated liposomes combined with TH302 for photodynamic therapy in triple negative breast cancer. *J Nanobiotechnology.* 2021;19(1):147. doi:10.1186/s12951-021-00891-8
31. Roberts-Dalton HD, Cocks A, Falcon-Perez JM, et al. Fluorescence labelling of extracellular vesicles using a novel thiol-based strategy for quantitative analysis of cellular delivery and intracellular traffic. *Nanoscale.* 2017;9(36):13693–13706. doi:10.1039/C7NR04128D
32. Liu Y, Zou Y, Feng C, et al. Charge conversational biomimetic nanocomplexes as a multifunctional platform for boosting orthotopic glioblastoma RNAi therapy. *Nano Lett.* 2020;20(3):1637–1646. doi:10.1021/acs.nanolett.9b04683
33. Hu Y, Wu X, Luo J, et al. Detection of pyrazinamide resistance of Mycobacterium tuberculosis using nicotinamide as a surrogate. *Clin Microbiol Infect.* 2017;23(11):835–838. doi:10.1016/j.cmi.2017.03.028
34. Yeo RW, Lai RC, Zhang B, et al. Mesenchymal stem cell: an efficient mass producer of exosomes for drug delivery. *Adv Drug Deliv Rev.* 2013;65(3):336–341. doi:10.1016/j.addr.2012.07.001
35. Geerickx E, Tulkens J, Dhondt B, et al. The generation and use of recombinant extracellular vesicles as biological reference material. *Nat Commun.* 2019;10(1):3288. doi:10.1038/s41467-019-11182-0
36. Melzer C, Rehn V, Yang Y, Bahre H, von der Ohe J, Hass R. Taxol-loaded MSC-derived exosomes provide a therapeutic vehicle to target metastatic breast cancer and other carcinoma cells. *Cancers.* 2019;11:6. doi:10.3390/cancers11060798
37. Shen Y, Pi Z, Yan F, et al. Enhanced delivery of paclitaxel liposomes using focused ultrasound with microbubbles for treating nude mice bearing intracranial glioblastoma xenografts. *Int J Nanomedicine.* 2017;12:5613–5629. doi:10.2147/IJN.S136401
38. de Castro RR, Do Carmo FA, Martins C, et al. Clofazimine functionalized polymeric nanoparticles for brain delivery in the tuberculosis treatment. *Int J Pharm.* 2021;602:120655. doi:10.1016/j.ijpharm.2021.120655
39. de Jong B, Barros ER, Hoenderop JGJ, Rigalli JP. Recent advances in extracellular vesicles as drug delivery systems and their potential in precision medicine. *Pharmaceutics.* 2020;12:11. doi:10.3390/pharmaceutics12111006
40. Huo C, Xiao J, Xiao K, et al. Pre-treatment with zirconia nanoparticles reduces inflammation induced by the Pathogenic H5N1 influenza virus. *Int J Nanomedicine.* 2020;15:661–674. doi:10.2147/IJN.S221667
41. Zhu L, Sun HT, Wang S, et al. Isolation and characterization of exosomes for cancer research. *J Hematol Oncol.* 2020;13(1):152. doi:10.1186/s13045-020-00987-y
42. Díaz-Perlas C, Oller-Salvia B, Sánchez-Navarro M, Teixidó M, Giralte E. Branched BBB-shuttle peptides: chemoselective modification of proteins to enhance blood-brain barrier transport. *Chem Sci.* 2018;9(44):8409–8415. doi:10.1039/C8SC02415D
43. Yang T, Martin P, Fogarty B, et al. Exosome delivered anticancer drugs across the blood-brain barrier for brain cancer therapy in Danio rerio. *Pharm Res.* 2015;32(6):2003–2014. doi:10.1007/s11095-014-1593-y
44. Matsumoto J, Stewart T, Banks WA, Zhang J. The transport mechanism of extracellular vesicles at the blood-brain barrier. *Curr Pharm Des.* 2017;23(40):6206–6214. doi:10.2174/1381612823666170913164738
45. Yang X, Shi G, Guo J, Wang C, He Y. Exosome-encapsulated antibiotic against intracellular infections of methicillin-resistant Staphylococcus aureus. *Int J Nanomedicine.* 2018;13:8095–8104. doi:10.2147/IJN.S179380
46. Zong J, Pollack GM. Modulation of P-glycoprotein transport activity in the mouse blood-brain barrier by rifampin. *J Pharmacol Exp Ther.* 2003;306(2):556–562. doi:10.1124/jpet.103.049452
47. Gupta D, Liang X, Pavlova S, et al. Quantification of extracellular vesicles in vitro and in vivo using sensitive bioluminescence imaging. *J Extracell Vesicles.* 2020;9(1):1800222. doi:10.1080/20013078.2020.1800222
48. Naftalin CM, Verma R, Gurumurthy M, et al. Coadministration of allopurinol to increase antimycobacterial efficacy of pyrazinamide as evaluated in a whole-blood bactericidal activity model. *Antimicrob Agents Chemother.* 2017;61:10. doi:10.1128/AAC.00482-17
49. Fang SB, Zhang HY, Wang C, et al. Small extracellular vesicles derived from human mesenchymal stromal cells prevent group 2 innate lymphoid cell-dominant allergic airway inflammation through delivery of miR-146a-5p. *J Extracell Vesicles.* 2020;9(1):1723260. doi:10.1080/20013078.2020.1723260
50. Kimiz-Gebologlu I, Oncel SS. Exosomes: large-scale production, isolation, drug loading efficiency, and biodistribution and uptake. *J Control Release.* 2022;347:533–543. doi:10.1016/j.jconrel.2022.05.027
51. Abhange K, Makler A, Wen Y, et al. Small extracellular vesicles in cancer. *Bioact Mater.* 2021;6(11):3705–3743. doi:10.1016/j.bioactmat.2021.03.015
52. Batrakova EV, Kim MS. Development and regulation of exosome-based therapy products. *Wiley Interdiscip Rev Nanomed Nanobiotechnol.* 2016;8(5):744–757. doi:10.1002/wnan.1395
53. David A. Peptide ligand-modified nanomedicines for targeting cells at the tumor microenvironment. *Adv Drug Deliv Rev.* 2017;119:120–142. doi:10.1016/j.addr.2017.05.006
54. Wen S, Dooner M, Papa E, et al. Biodistribution of mesenchymal stem cell-derived extracellular vesicles in a radiation injury bone marrow murine model. *Int J Mol Sci.* 2019;20:21. doi:10.3390/ijms20215468
55. Fabbri M. Natural killer cell-derived vesicular miRNAs: a new anticancer approach? *Cancer Res.* 2020;80(1):17–22. doi:10.1158/0008-5472.CAN-19-1450